

Development of Human Hip Capsule Finite Element Model

Nataraju Vusirikala

Senior Researcher, General Motors Global R & D

This paper has not been screened for accuracy nor refereed by any body of scientific peers and should not be referenced in the open literature.

ABSTRACT

The current study focuses on the development of a finite element model of the hip capsule ligament to represent the joint between the femur and the pelvis. The finite element model of the hip capsule is represented as comprising of eight sectors, consisting of the important ligaments in those regions of the capsule. The geometric parameters for the capsule are determined from available literature. A soft tissue material model is used to represent the nonlinear behavior of the capsule ligaments. Available hip distraction test data is used to validate the finite element model. A parametric study is conducted with the isolated capsule sector finite element model to understand the effects of different material parameters on the tensile load-deflection response of the capsule. The material properties for each sector of the hip capsule are systematically estimated to match the corresponding values from isolated capsule sector tensile tests reported in the literature. A verification exercise for the sector hip capsule material properties is carried out by considering a setup comprising an integrated pelvis-hip- capsule-femur finite element model and comparing with data available from hip distraction tests in the literature. The stiffness of the hip capsule finite element model is found to lie within the reported test corridor from hip distraction tests. The developed hip capsule finite element model will be of use in examining the stresses and strains in the joint ligaments.

INTRODUCTION

The pelvis is one of several human body regions that are susceptible to injury in the event of an automobile impact [Teresinski, 2001, Aekbote et al., 2003, Kuppa and Fessahaie, 2003, Rupp and Schneider, 2004, Sochor and Rupp, 2005]. The simulation and prediction of such injuries requires the use of detailed computer models. One of the challenges of developing such computer models is in the accurate representation of

various human body joints in these models. Several contemporary computer models (e.g. Anthropometric Test Device (ATD) Models, ESI's H-Model [Choi et al., 1999], the GM-UVA Human Body Model [Deng, 2007]), intended to simulate the human body in an automobile impact scenario, represent the connection between the pelvis and the femur head by a simplified rigid kinematic joint, with appropriate mechanical properties (joint stiffness in various directions). Such a representation limits injury prediction in the pelvis region on account of the requirement of typical finite element software like LS-DYNA [LS-Dyna, 2006] for the connecting bodies (ilium and femoral head) to be rigid. A natural progression towards accurate representation of the hip capsule is through 1-D elements. Vezin et al. [Vezin and Verriest, 2005] idealized the hip capsular ligament as a set of 1-D elements in the HUMOS model. While this constituted a step forward from the idealized rigid kinematic joint, this model could not be used to perform detailed stress analysis in the capsule region, or to predict phenomena like capsule laxity, ligament tear, etc. [Teresinski, 2001, Philippon and Schenker, 2005]. Stewart and co-workers [Stewart et al., 2004] developed a model of the hip capsular ligament with solid elements and experimentally obtained tissue material properties for simulating total hip arthroplasty (THA) applications. One advantage of representing the hip capsule in the model as soft tissue is the more accurate capture of the load transfer mechanism between the pelvis and the lower extremity in comparison to rigid kinematic joints or 1-D beam representations. This could turn out to be significant for a dynamic load case like pedestrian impact.

The hip joint is essentially a ball and socket joint wherein the ligaments and the contact interface between the acetabulum and the femur head constrain the femur head (ball) from slipping out of the acetabulum (socket). The hip capsule is an important part of the hip joint that allows for joint articulation and provides stability. The hip capsule is strengthened by three important ligaments, namely—the iliofemoral ligament, the ischiofemoral ligament and the pubo-capsular ligament [Gray and Carter, 1995]. The elastic behavior of the ligament soft tissue allows for flexion, abduction and internal rotation of the lower extremities about the hip joint. Several studies [Wingstrand and Wingstrand, 1997, Scifert et al., 1999] have been carried out to understand hip joint biomechanics, but these have been focused more on sport related injuries and total hip arthroplasty (THA). To date, the availability of hip capsule response data in a dynamic impact scenario is very limited.

The availability of relevant material data comprises one of the most significant prerequisites for building accurate finite element (FE models). Until recently, not much data has been published regarding mechanical properties of the hip capsule. Hewitt et al., 2000 performed the first set of tests to understand the material behavior of the important ligaments in the hip capsule. They carried out tensile tests on cadaveric ligament specimens to failure. Several important properties like stress and strain at failure, toe-region and linear region elastic modulus were documented. They also reported the variation of cross-sectional area of the ligaments along the fiber direction (from the acetabulum side to the femoral side). Their study highlighted the mechanical heterogeneity of the hip capsule. It was observed in their tests that the iliofemoral ligament (anterior region of the capsule) was stiffer than the ischiofemoral ligament (posterior region of capsule). However these tests were limited only to key capsule ligaments like the ischiofemoral, iliofemoral and pubofemoral ligaments. This study was also performed at low rates to avoid visco-elastic effects.

Stewart et al., 2002 performed more detailed tests on the whole hip capsule instead of a few important hip capsule ligaments. They reported regional material and geometrical properties of the whole human hip capsule ligament. Distraction tests were performed on cadaveric specimens to calculate the stiffness of the whole hip capsule ligament. After each test the whole capsule was cut into several sectors and subjected to tensile load until failure to calculate the stiffness of each sector of the capsule. The sectors were carefully cut so as to not cut across ligament fibers. This study reported several mechanical properties of the capsule like stiffness and failure load of each capsule sector, typical load-deflection curves for the whole capsule and individual sectors for distraction and tensile tests respectively. They also performed tests at various distraction rates but concluded that strain rate effects were insignificant for their load case. However, other studies [Kemper et al., 2007] have reported strain rate effects in testing the iliofemoral and ischiofemoral ligaments.

Stewart et al., 2004 used some of their own test data [Stewart et al., 2002] to build finite element models to simulate total hip dislocation. They reported significant improvement in the FE model joint behavior. The

focus of the current work is to develop a hip capsule ligament model similar to the one developed in [Stewart et al., 2004], but for eventual application to occupant and pedestrian impact scenarios.

The current study focuses on the development of a finite element model of the hip capsule ligaments for a human body model representative of a 50th percentile male. This model is further used to connect the femur to the pelvis. A recently developed material model [LS-DYNA, 2006] for soft tissue, which takes into account viscoelastic effects as well as tissue fiber direction, is used for the ligament model. As a first step, a validated FE model was developed to simulate the individual capsule sector tensile test. Parametric studies were conducted using this model to identify the most important tissue material parameters which influence the capsule stiffness. Subsequently, the material parameters of each sector were estimated. The second step involved the development of a FE model to simulate a hip distraction test. The sectoral material properties obtained in the first step were used to develop a whole hip capsule model to simulate hip distraction test. These FE results verified the estimated material properties of individual capsule sector in the previous step. The integrated hip capsule FE model was further used to conduct a brief parametric study by varying capsule material model parameters. This study provides a glimpse of the influence of material model parameters on overall load-deflection behavior of the hip capsule.

METHODS

Hip capsule geometry

The hip capsule is a dense fibrous tissue with the shape of a cylindrical sleeve. It spans the circumference of the acetabulum rim along the medial end. The other end of the capsule surrounds the neck of the femur. It is attached anteriorly, to the intertrochanteric line, posteriorly to the lower part of the neck closer to lesser trochanter, superiorly and inferiorly to the base of the femur neck [Gray and Carter, 1995]. The thickness of the tissue varies both along the circumference and length of the capsule. The fiber directions vary in different parts of the capsule. There are three dominant dense regions which are identified as the iliofemoral ligament, the ischiofemoral ligament and the pubofemoral ligament. It is very difficult to identify the distinct boundaries of these ligaments and therefore it is better to model the ligaments as a single unified capsule model. The iliofemoral ligament part of the capsule is the thickest and has its fibers run longitudinally. The anterior region is the thinnest and weakest part of the capsule.

Stewart et al., 2002 have reported circumferential variation of capsule geometric parameters (length, thickness). They have dissected each of ten cadaveric hip joint specimens into eight sectors and reported the range of these geometric parameters. The average values from this study were taken as the basis for building the FE mesh for the capsule FE model. Variation across the length of the capsule was also considered based on the geometric data provided in Hewitt et al., 2000. The insertion points of various ligaments were obtained from [Gray and Carter, 1995, and Stewart et al., 2002] and were mapped onto a pelvis-femur FE model [Untaroiu et al., 2005, Deng, 2007]. Figure 1 shows the identified insertion points. Figure 2 shows the posterior view of the hip capsule FE model. The eight different sectors as dissected by Stewart et al., 2002 and corresponding fiber directions are also shown in Figure 2. The thickness variation of capsule along the circumference is also captured in the FE model. In general it can be observed that sector 1 represents the pubofemoral ligament, sectors 2-4 represent the femoral arcuate and posterior regions of capsule, sectors 5-6 represent the ischiofemoral ligament, sector 7 is the superior iliofemoral ligament and sector 8 is the inferior iliofemoral ligament.

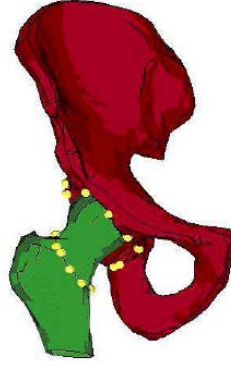


Figure 1: Insertion Points – anterior view

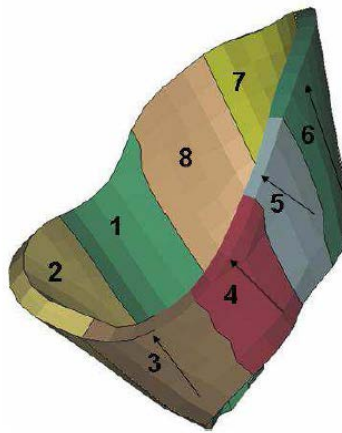


Figure 2: Whole Hip Capsule – posterior view

Capsule material model

Accurate capture of the ligament mechanics necessitates the use of appropriate material models for the capsule model. As reported in earlier studies [Hewitt et al., 2002, Stewart et al., 2002] the hip capsule tissue behaves in a highly nonlinear manner. A recently developed advanced tissue material model is used in LS-DYNA® to represent the capsule. The material model (MAT_SOFT_TISSUE_VISCO [LS-DYNA, 2006]) is based on a viscoelastic model proposed by Puso and Weiss [Puso and Weiss, 1998], and is a transversely isotropic (stiffer in the fiber direction) hyperelastic model for representing biological soft tissues like the capsule ligament. The constitutive model provides an isotropic Mooney-Rivlin mix reinforced by fibers. The overall strain energy (W) is uncoupled and includes two isotropic deviatoric ground substance (matrix) terms, a fiber term (F), and a bulk term as given below in Equation 1 [Puso and Weiss, 1998].

$$W = C_1(\bar{I}_1 - 3) + C_2(\bar{I}_2 - 3) + F(\lambda) + \frac{1}{2}K[\ln(J)]^2 \quad (1)$$

Here I_1, I_2 are the deviatoric invariants of the right Cauchy deformation tensor, λ is the deviatoric part of the stretch along the current fiber direction, and J is the volume ratio. The material coefficients C_1, C_2 are the Mooney-Rivlin coefficients and K is the effective bulk modulus. The derivatives of the fiber term F are defined as a function of fiber stretch to capture the behavior of crimped collagen as given below in equation 2. The fibers are assumed to be unable to resist compressive loading when λ is less than 1. An exponential function describes the straightening of the fibers, while a linear function describes the behavior of the fibers once they are straightened past a critical fiber stretch.

$$\begin{aligned} \bar{\lambda} \frac{\delta F}{\delta \lambda} &= 0, & \bar{\lambda} &\leq 1 \\ \bar{\lambda} \frac{\delta F}{\delta \lambda} &= C_3 [\exp(C_4(\bar{\lambda} - 1)) - 1], & 1 &\leq \bar{\lambda} \leq \lambda^* \\ \bar{\lambda} \frac{\delta F}{\delta \lambda} &= C_5 \bar{\lambda} + C_6, & \bar{\lambda} &\geq \lambda^* \end{aligned} \quad (2)$$

The parameter C_3 scales the exponential stress, C_4 specifies the rate at which collagen straightens, C_5 is the modulus of straightened fibers, and λ^* is the critical fiber stretch at which the fibers are straightened. C_6 is determined to ensure stress continuity at λ^* . Apart from these parameters the LS-DYNA material model also allows co-ordinate system input for defining the fiber direction in each element. This is very important considering the different fiber directions in different sectors of the capsule as shown in Figure 2.

Figure 3 shows typical load-deflection responses from tensile tests on a capsule tissue sector reported by Stewart et al., 2002 and Hewitt et al., 2002. The curves are initially flat (toe region) followed by exponential rise in stiffness and eventually have a linear slope region. The material model described above is therefore well suited to model the capsule tissue behavior. It can also be seen in the figure that different parts of the capsule have different stiffness. The curves corresponding to the superior and inferior iliofemoral ligament, the ischiofemoral ligament and the femoral arcuate ligament from Hewitt et al., 2002 have two major differentiators: the slope of the linear portion of the curve and the initiation point for exponential rise in stiffness. The heterogeneity of capsule tissue is more evident in Figure 4; it shows the variation in tangent structural stiffness of each sector across the ten capsule specimens as reported by Stewart et al., 2002.

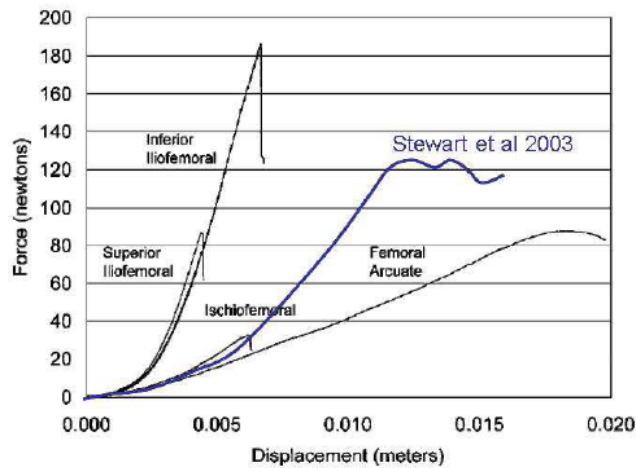


Figure 3: Load Deflection Curves for ligament tensile test from [Stewart et al., 2002 and Hewitt et al., 2002]

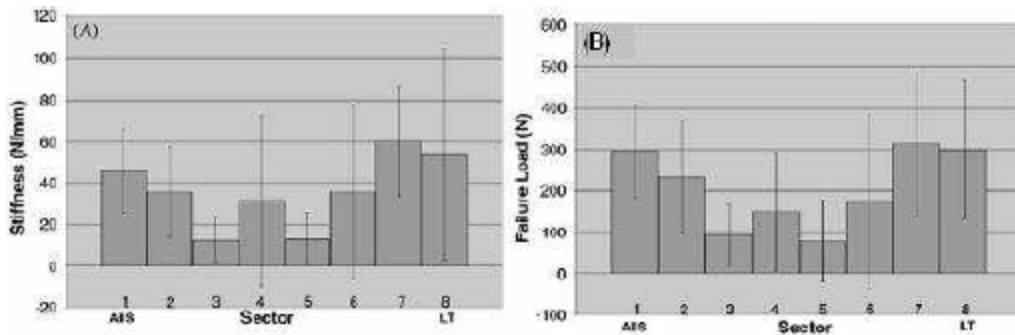


Figure 4: Spatial Distribution of Capsule Material Properties (A – Tangent Structural Stiffness, B – Ultimate Load at Failure) [Stewart et al., 2002]

In the current study, the capsule material properties are estimated and verified in two separate stages. In the first stage the material properties for each of eight individual sectors of the capsule were estimated using isolated sector tensile test data (Stewart et al., 2002) and verified in the next stage using hip distraction test data (Stewart et al., 2002).

Isolated sector material properties

A FE model was developed to simulate an isolated sector tensile test conducted by Stewart et al., 2002. The dimensions of the representative capsule sector specimen are 45mm x 15mm x 5mm. All finite element simulations were carried out using LS-DYNA® (LS-DYNA, 2006) with hexahedral elements. A convergence study was carried out to obtain the requisite mesh densities for the test setup, and the final mesh consisted of 400 elements and 700 nodes. The tissue was clamped at both ends to rigid blocks. The bottom rigid block was constrained in all directions and a unidirectional tensile load was applied at a rate of 4mm/s to the top end. This FE model represents the tensile tests carried out by Stewart et al., 2002 on all the sectors of the capsule.

Table 1: Initial Material Properties

Bulk Modulus (GPa)	C1 (GPa)	C1 (GPa)	C1 (GPa)	C1	C1 (GPa)	λ^*
4.315	6.2e-5	0	4.2e-03	158.9	0.2793	1.06

Table 2: Material Parameter Variation

Parameter	Base	1	2
C₁ (GPa)	1.2e-4	3.6e-4	4.0e-5
C₃ (GPa)	1.0e-5	1.0e-4	1.0e-6
C₄	6.9	1.4	34.5
C₅ (GPa)	0.0185	0.01	0.0285
λ^*	1.07	1.04	1.14
Bulk Modulus (GPa)	4.315	43.15	0.4315
Load rate (mm/s)	4	0.4	0.04

The material parameters for a base FE model were obtained by comparing the load deflection response from the model with a representative Stewart et al., 2002 test response (Figure 3). Before carrying out the material property estimation process, a parametric study was conducted using the above mentioned representative isolated sector FE model to understand the influence of several material model parameters on the load-deformation characteristic of various tissue sectors. The material parameters studied were the bulk modulus (K), the hyperelastic coefficients (C_1 , C_3 , C_4 , C_5) and the critical fiber stretch (λ^*). The effects of varying load rate were also studied using the FE model. Each parameter is varied exclusively at a time from base material properties as shown in Table 2. The results are discussed in the next section.

Some of the observations from the parametric study are expected because of the inherent nature of the defined material model. The present study further strengthens the understanding of the model behavior and also throws light on the qualitative influence of each parameter on the load-deflection response. This knowledge was further used in the material properties estimation procedure. The estimation procedure

followed is shown in Figure 5. The initial material properties of the tissue are given in Table 1. An iterative process (Figure 5) is used to estimate the material model parameters for tissue response curves from Stewart et al., 2002, Hewitt et al., 2002). Figure 6 shows a very good match between FE and test responses (Stewart et al., 2002, Hewitt et al., 2002) and hence validates the FE model of the isolated sector tensile test. Different material parameter sets were obtained for matching each test response curve shown in Figure 3. It has to be noted that tissue material is generally very soft and has high deformation for a given load (maximum of 100N in this case). One of the issues raised during FE simulation using LS-DYNA is the high ratio of hourglass energy to internal energy. This ratio was controlled by carefully estimating hourglass control parameters and by refining the FE mesh.

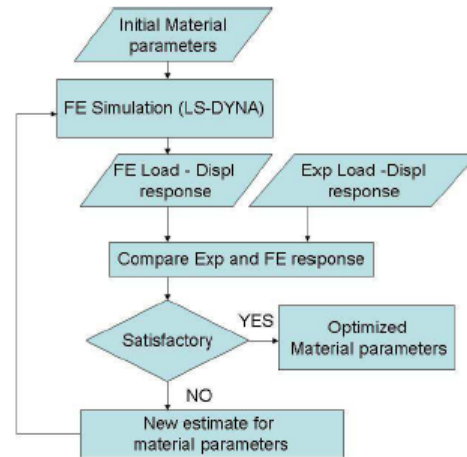


Figure 5: Iterative Process to Estimate Tissue Parameters

Table 3: Target FE model sector stiffness and the reported test sector stiffness Stewart et al., 2002

Sector	FE Target Stiffness N/mm	Average	Upper	Lower
1	29	45	70	20
2	16	36	58	14
3	8	12	24	0
4	14	31	75	-13
5	10	12	24	0
6	23	36	80	-8
7	39	60	88	32
8	35	54	105	3

The material set corresponding to the Stewart et al., 2002 response curve (Figure 3) was taken as the base parameter set (first column of Table 2) to estimate the properties of all eight sectors of the capsule. It can be seen from the test responses (Figure 3) and Figure 4 that the main differentiator for different sectors is the stiffness in the linear region of the response. The stiffness in the linear region is dependent largely on the parameter C_5 . Additionally, the test responses from Hewitt et al., 2002 suggest that the initiation of exponential rise in stiffness in the iliofemoral ligament is early compared to the ischiofemoral and femoral arcuate ligaments. This can be controlled using the critical fiber stretch (λ^*) parameter

The next step is to estimate material parameter sets for different sectors corresponding to Stewart et al. test results (Figure 4). The estimation procedure shown in Figure 5 is used and C_5 and λ^* parameters were varied to get final material sets for all sectors of the capsule. Table 3 shows the comparison of target FE model sector stiffness and the reported test sector stiffness. The target sector stiffness was chosen in such a way that each sector stiffness lies within the reported test range and also the sum of sector stiffness lies in the reported test range. The general trend observed from sector one to sector eight in the test data (Stewart et al., 2002)

was also used a guideline while choosing the target sector stiffness. The final estimated individual sector properties are shown in the results section.

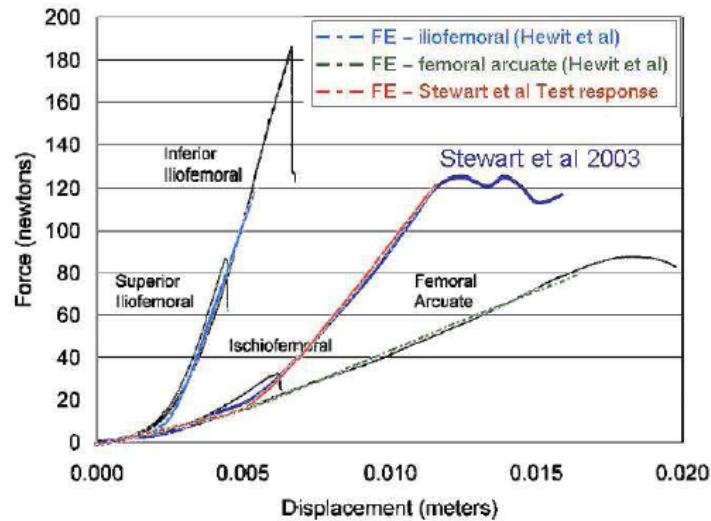


Figure 6: Comparison of load-deflection response of FE model and test data from [Stewart et al., 2002] and [Hewitt et al., 2002]

Integrated Capsule FE Model

The next stage is to verify the estimated capsule material properties. An integrated hip capsule-pelvis-femur model was developed to verify the capsule sector material properties estimated above and to understand the behavior of the capsule in an integrated setup with pelvis and femur finite element models. In a pedestrian impact scenario there is essentially hip distraction combined with loads to abduct the joint.

Owing to paucity of reported test data, only the hip distraction load case is being examined in the current study. However, this is not expected to limit the use of the current FE model, since the capsule ligament model was developed systematically through validation of the individual sectors of the hip capsule ligament.

The FE model used to simulate hip distraction tests performed by Stewart et al., 2002, together with the test schematic is shown in Figure 7. The iliac crest and ischial tuberosity are completely constrained. The distal portion of the femur is potted in a cup which is used to apply the load through MTS servo-hydraulic materials testing machine at a distraction rate of 0.4 mm/s upto a maximum of 750N. The peak load was chosen as to not injure the capsule. The longitudinal axis of the femoral neck (and hence the capsule) is coincident with the direction of the applied tensile force. The arrow mark in Figure 7 shows the direction of applied load. The applied load and the displacement of the loader are recorded. In the present study the FE model responses (load-displacement) were compared to the corresponding test responses to verify the integrated capsule property.

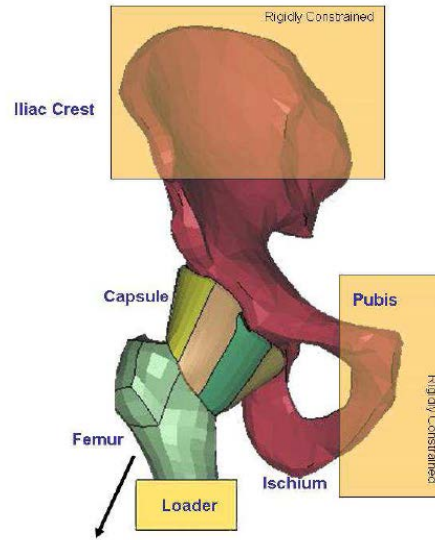


Figure 7: FE model to simulate hip distraction test

The pelvis and femur FE models were obtained from earlier studies reported by Deng, 2007 and Untaroiu et al., 2005. The cartilage and lunata surface are modeled as an interface between the femur and pelvis bones. Contacts are defined between femur and cartilage, cartilage and lunata surface, lunata surface and pelvis. The material properties for cartilage and lunata surface are obtained from Athanasiou et al., 1995. Adjoining capsule sectors share common nodes at the junction. The capsule nodes are tied to the acetabulum rim at the medial end and tied to the femur neck at the lateral end. Each sector is given different material properties as estimated in the previous section.

RESULTS

Isolated sector parametric study

Some observations from the parametric study conducted with the above mentioned representative isolated sector FE model are mentioned below:

- The slope in the initial toe region is dependent on the bulk modulus and C_1 .
- λ^* defines the point at which the linear stiffness region commences.
- C_5 is the most important parameter to capture the tangent structural stiffness (slope in the linear region of the response).
- A special case was studied where $C_5 = 0$. The tissue does not stiffen after critical fiber stretch for this particular case.
- It is observed that there is a linear relationship between C_5 and tangent structural stiffness. Figure 8 shows the data points corresponding to C_5 parametric study cases. The fitted linear trend line equation is also shown here.

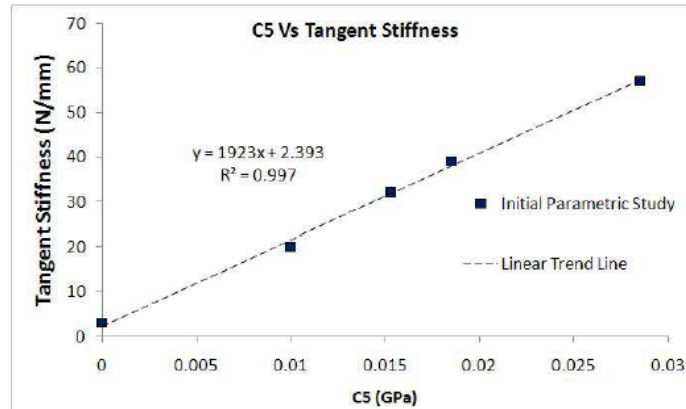


Figure 8: C_5 vs. tangent structural stiffness

Capsule sector material properties

The resultant load-deflection responses for the eight sectors of the capsule corresponding to the target stiffness (Table 3) are shown in Figure 9. The material sets (Bulk Modulus K , hyperelastic coefficients (C_1 , C_3 , C_4 , C_5), (λ^*)) corresponding to these responses for all eight sectors of the capsule were further used in the integrated capsule FE model.

Integrated Capsule FE Model

Figure 10 shows the typical load-displacement response from distraction test conducted by Stewart et al., 2002. It can be seen that the right hip joint is very soft compared to the left hip. There is no reason mentioned in their study for this particular behavior. They reported that of the 10 tests conducted (left and right hip joints for 5 subjects) the intra-subject (between right and left hip joints for the same subject) variability approached inter-subject variability. Hence, the individual hip joints were considered as ten separate specimens. The comparison of load-displacement response of FE model and test is shown in Figure 10. It should be noted that the test response curves are from two tests only and do not represent the total test corridor. The FE response curve matches well with one of the test response curves. The FE model tangent structural stiffness value of 145.1 N/mm is well within the reported (Stewart et al., 2002) range of 155.2 ± 29.1 N/mm (corridor obtained by considering all the tests). The loading of different sectors is largely dependent on the direction of the applied load. In this particular case, sectors five and three have the highest load. The same conclusion can be interpreted from the strain distribution contour as shown in Figure 11.

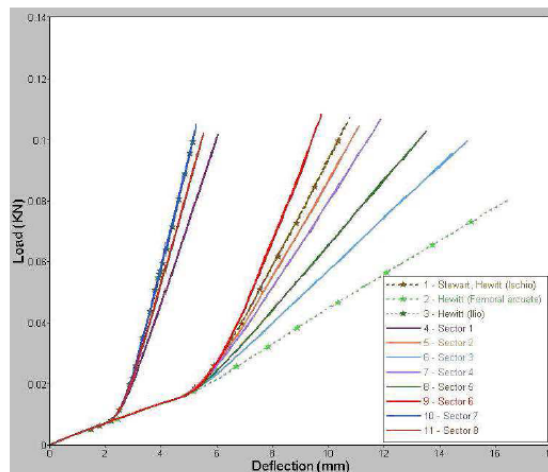


Figure 9: FE response for all eight sectors of the capsule

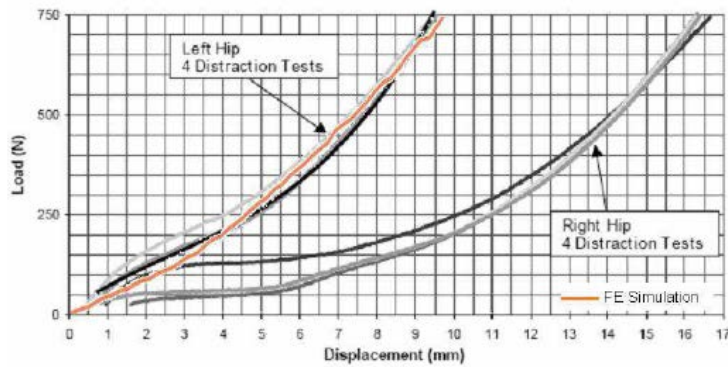


Figure 10: Representative load-displacement curve from hip distraction test [Stewart et al., 2002] and corresponding FE simulation

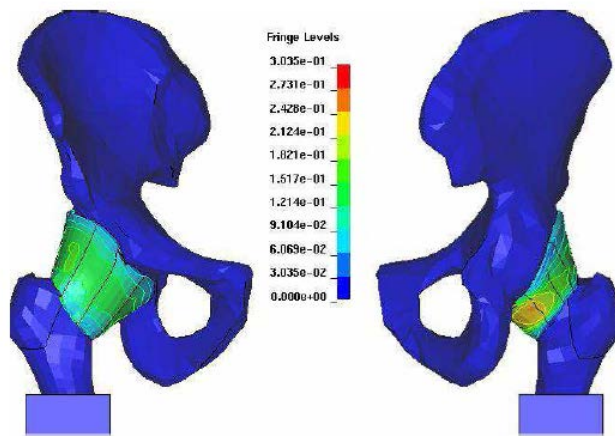


Figure 11: Strain distribution in the capsule at an intermittent time step for the hip distraction test

It has to be noted that the capsule model response is dependent on individual sector properties. The sector properties have a range of stiffness and the current material properties are based on target FE stiffness (Table 3) for each sector. Stewart et al., 2002 reported a variation of 30% in sum of individual sector stiffness (138.1 ± 44.2). In Figure 8: C_5 vs. tangent structural stiffness it was observed that the tangent structural stiffness of individual capsule is linearly varying with C_5 parameter. Therefore a brief parametric study was conducted to understand the influence of variation of C_5 parameter (as shown in Table 4) on capsule response. Figure 12 highlights the influence of C_5 on whole capsule behavior. The tangent structural stiffness of whole hip capsule FE model increases by about 21% for Case 1, and decreases by about 23% for Case 2. A more detailed uncertainty analysis of hip capsule material properties is planned for the future.

Table 4: Variation in Parameters

Case 1	Increasing C_5 by 30% for all sectors
Case 2	Decreasing C_5 by 30% for all sectors

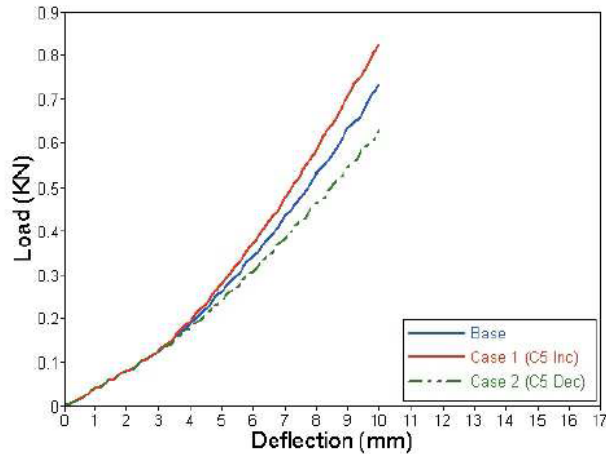


Figure 12: Parametric study for using hip distraction FE model

CONCLUSIONS

A finite element model of the whole hip capsule was developed. The material properties of individual sectors of the capsule were estimated from isolated sector tensile test data. There is a wide range in the reported stiffness of each capsule sector. Target stiffness for each capsule was chosen based on the reported range of individual capsule sector stiffness and whole capsule stiffness data. Material model parameters of eight sectors of capsule were estimated based on these target FE stiffness data. This material data was further used to model the whole capsule. The whole capsule was integrated with pelvis and lower extremity (partial femur only). The integrated model was used to model a hip distraction test and the load-displacement responses from Stewart et al., 2002 hip distraction tests was used to verify the estimated sector material properties. The FE response compares well with one of the test responses from hip distraction tests. The estimated tangent structural stiffness of the FE model lies well within the reported test corridor range. It has to be noted that the FE response is largely dependent on the chosen material properties of different capsule sectors. A brief parametric study was done to show the influence of different material model parameters. The loading pattern of different capsule sectors is largely dependent on the applied load direction. The capsule model is validated only for distraction case. However as the capsule sectors were validated individually, the present model may also be used for other load cases like pedestrian impacts.

REFERENCES

- AEKBOTE, K., SCHUSTER, P., KANKANALA, S., SUNDARARAJAN, S., ROUHANA, S., (2003), The biomechanical aspects of pedestrian protection, *International Journal of Vehicle Design* 32, pp. 28-52.
- ATHANASIOU, K., AGARWAL, A., DZIDA, F., (1995), Comparative study of the intrinsic mechanical properties of the human acetabular and femoral head cartilage, *Annals of Biomedical Engineering* 23, pp. 697-704.
- CHOI, H., EOM, H., KHO, S., LEE, I., (1999), Finite element human model for crashworthiness simulation, *Soc. of Automotive Engineers, SAE 1999-01-1906*.
- DENG, B., (2007), Human model for real-world vehicle-pedestrian impact simulations Tech. Rep., *Human Modeling and Simulation in Automotive Safety, ENSAM de Paris*.

- GRAY, H., CARTER, H., (1995), Gray's Anatomy, Barnes & Noble Publishers.
- HEWITT, J., GLISSON, R., GUILAK, F., VAIL, T., (2000), Regional material properties of human hip joint capsule ligaments, *J. of Ortho. Res.*, 19, pp. 359-364.
- HEWITT, J. D., GLISSON, R. R., GUILAK, F., VAIL, T., (2002), The mechanical properties of the human hip capsule ligaments, *J. Arthroplasty*, 17 (1), 82-89.
- KEMPER, A., CRAIG, M., SMITH, B., DUMA, S., (2007), Quasi-linear viscoelastic characterization of human hip ligaments, *Biomedical Sciences Instrumentation* 43, pp. 324-329.
- KUPPA, S., FESSAHAIE, O., (2003), Overview of KTH injuries in frontal crashes in the US, 18th ESV Conference.
- LS-DYNA, (2006), LS-DYNA Version 971 Keyword Users Manual. LSTC Corp Ltd.
- PHILIPPON, M., SCHENKER, M., (2005), Athletic hip injuries and capsular laxity, *Operative Techniques in Orthopaedics*, 15, pp. 261-266.
- PUSO, M., WEISS, J., (1998), Finite element implementation of anisotropic quasilinear viscoelasticity using a discrete spectrum approximation, *ASME J. of Biomech Engg* 120, pp. 62-70.
- RUPP, J., SCHNEIDER, L., (2004), Injuries to the hip joint in frontal motor-vehicle crashes: Biomechanical and real-world perspectives, *Orthopedic Clinics of North America*, 35, pp. 493-504.
- SCIFERT, C., BROWN, T., LIPMAN, J., PEDERSEN, D., HEINER, A., CALLAGHAN, J., (1999), Development and physical validation of a finite element model of total hip dislocation, *Computer Methods in Biomechanics and Biomedical engineering*, 2, pp. 139-147.
- SOCHOR, M., RUPP, J., (2005), Knee-Thigh-Hip injuries in frontal crashes, *Annals of Emergency Medicine*, 46, pp. 168-171.
- STEWART, K., EDMONDS-WILSON, R., BRAND, R., BROWN, T., (2002), Spatial distribution of hip capsule structural and material properties *J. of Biomech.* 35, pp. 1491-1498.
- STEWART, K., PEDERSEN, D., CALLAGHAN, J., BROWN, T., (2004), Implementing capsule representation in a total hip dislocation finite element model, *The Iowa Orthopaedic Journal* pp. 1-8.
- TERESINSKI, G., (2001), Pelvis and hip joint injuries as a reconstructive factors in car-to-pedestrian accidents, *Forensic Science International*, 124, pp. 68-73.
- UNTAROIU, C., DARVISH, K., CRANDALL, J., DENG, B., WANG, J., (2005), A finite element model of the lower limb for simulating pedestrian impact *Stapp Car Crash Journal* 49, pp. 157-181.
- VEZIN, P., VERRIEST, J., (2005), Development of a set of numerical human models for safety, 19th ESV Conference
- WINGSTRAND, H., WINGSTRAND, A., (1997), Biomechanics of the hip joint capsule - A mathematical model and clinical implications, *Clinical Biomechanics* 12, pp. 273-280.